Designing Nanoparticle Translocation through Membranes by Computer Simulations

ARTICLE *in* ACS NANO · FEBRUARY 2012

Impact Factor: 12.88 · DOI: 10.1021/nn2038862 · Source: PubMed

3 AUTHORS, INCLUDING:

Wen-de Tian
Suzhou University
20 PUBLICATIONS **347** CITATIONS

SEE PROFILE

Designing Nanoparticle Translocation through Membranes by Computer Simulations

Hong-ming Ding,[†] Wen-de Tian,[‡] and Yu-qiang Ma[†,‡,*]

[†]National Laboratory of Solid State Microstructures and Department of Physics, Nanjing University, Nanjing 210093, China and [‡]Center for Soft Condensed Matter Physics and Interdisciplinary Research, Soochow University, Suzhou 215006, China

ABSTRACT

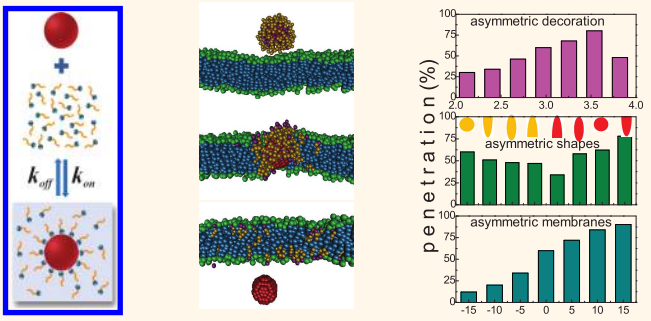

Nanoparticle penetration into cells is an important process in drug/gene delivery. Here, we successfully design one type of novel nanoparticles with ligands decorating its surface by dynamic bonds and find that the nanoparticle can spontaneously penetrate through membranes by using dissipative particle dynamics simulations. Moreover, the physical parameters of both ligands (for example, ligand type and density) and nanoparticles (such as size and shape) have significant effects on penetration efficiency and translocation time. Especially for nanoparticles with anisotropic shapes or asymmetric surface decoration, the penetration efficiency may reach about 80%. We also provide insights into the interaction between nanoparticles and asymmetric membranes and find that the membrane asymmetry can even increase the penetration efficiency to above 90%. The present study suggests a potential way to translocate novel nanoparticles through membranes, which may provide new ideas for future experimental nanoparticle design and drug delivery.

KEYWORDS: nanoparticle · lipid membrane · translocation · cytotoxicity · computer simulation

Nowadays, nanomaterials are widely used in biotechnology.[1,2] Their applications in biomedicine, such as drug delivery and gene carriers, are very promising.[3,4] Therefore, understanding the interactions between nanomaterials and biomembranes,[5−8] for example, how nanoparticles cross the cell membrane and enter into the cell interior,[9−13] is of central importance for their potential applications.

It is now realized that endocytosis and direct penetration (diffusion) are two main ways to translocate nanoparticles through membranes.[8,10,11] Large particles whose sizes are in the range of tens to hundreds of nanometers usually cross the membrane by endocytosis.[4,12,13] This progress can be divided into three parts:[12−14] first particles sticking to the membrane, second the membrane wrapping the particle, and finally the pinch-off (particle−lipid complex detaching from the membrane). However, for small particles whose diameters are just several nanometers or even smaller,[12,13,15] endocytosis is no longer an effective way because the decrease in adhesion energy which mainly comes from receptor−ligand interaction may not balance out the increase in bending energy and stretching energy that originate from membrane deformation. In this case, nanoparticles may aggregate in order to be endocytosed.[16] Another useful method is to decorate some types of ligands like PEG or MUS on nanoparticles' surface,[11,17] which can also make nanoparticles internalized by endocytosis. However, endocytosed nanoparticles by constructing the membrane-bound vesicles are confined in the endosomes and may not be able to get out of vesicles and reach the cytosol.[7] In this sense, the direct penetration of nanoparticles into cells is a better way because there are no lipids coated on their surfaces. Unlike small molecules such as O_2 and CO_2, however, nanoparticles cannot cross membranes by diffusion on their own. Although adding an external force on the nanoparticle can help its penetration,[10,18] the practical applications will be limited. Some nanoparticles like dendrimers can induce pore formation in membranes,[19−22] which can also make direct penetration possible. However, membranes are disrupted more or less by pore formation. If the membrane disruption is too strong, it may even cause cell death.[5,8] So, it is a challenging

* Address correspondence to myqiang@nju.edu.cn.

Received for review October 9, 2011 and accepted January 1, 2012.

Published online January 01, 2012
10.1021/nn2038862

and promising problem to design such nanoparticles that can spontaneously penetrate through membranes and have little effect on membranes and their own functions. To our best knowledge, there are few papers studying these problems, especially for designing such small nanoparticles with high penetration efficiency by diffusion. Here, for the purpose of effectively translocating nanoparticles through membranes, we apply dissipative particle dynamics (DPD) simulations (see details in the Methods section) to design one type of such novel nanoparticles and examine their ability to deliver the cell membrane under the symmetric and asymmetric cases of both nanoparticles and membranes.

In our simulations, each amphiphilic lipid consists of a headgroup containing three connected hydrophilic beads and two tails with respective four hydrophobic beads (see Figure 1a). When lipids are immersed in water, they can form a stable, tensionless membrane (see Figure S1 in Supporting Information). A ligand is composed of four connected beads, three of which are hydrophobic and the other one is a hydrophilic head (see Figure 1a). The nanoparticle can be fabricated by arranging the hydrophilic DPD beads (P) on an fcc lattice with lattice constant $\alpha = 0.30$ nm into a desired geometry shape and volume.

RESULTS AND DISCUSSION

The hydrophilic/hydrophobic property of nanoparticles is an important factor in their interaction with membranes. Hydrophilic nanoparticles could attach to the membrane (see Figure S2.a in Supporting Information), due to the lipid headgroup−nanoparticle interaction.[23] When the interaction is strong enough, the membrane can totally engulf the nanoparticle, similar to the endocytosis process.[14] Unlike hydrophilic nanoparticles, hydrophobic nanoparticles such as fullerenes[24] and nanotubes[25] can insert into membranes because they prefer lipid tails. If we decorate hydrophobic chains onto the hydrophilic surface of nanoparticles, they can also insert into membranes (see Figure S2.b in Supporting Information), which was observed in experiments.[26] However, in general cases, nanoparticles staying in membranes, but not entering into the cell interior, may somewhat disrupt the membrane and can even cause cell death.[5,8] Here, we design one new type of nanoparticles by combining the former two properties, that is, decorating ligands on the nanoparticle's surface by dynamic bonds.[27] The dynamic bond is defined as any class of bond that can selectively undergo reversible breaking and reformation, usually under equilibrium conditions. It can generally be divided into two types:[27] dynamic covalent bond and noncovalent dynamic bond. Dynamic covalent bond cannot access its reversibility without a catalyst (or stimulus), while noncovalent dynamic bond is highly susceptible to thermal conditions, solvents/reagents, and concentrations. In our simulations, we adopt the reversible noncovalent dynamic bonds to generate the aggregation and detachment process between nanoparticle and ligands (see Figure 1b) by the following rule: when the bond length between the arbitrary bead of the nanoparticle and the bead of ligand head is longer than its initial length, the bond is broken with a probability being P_{off}, and when the length is shorter than its initial length, the bond forms with a probability P_{on}. We find that the ratio $P_a = P_{on}/P_{off}$ can well replace the reaction equilibrium constant $K_a = k_{on}/k_{off}$, which determines the final balance of the nanoparticle−ligand complex[28] (see Figures S3 and S4 in Supporting Information). When solvents are hydrophobic, the nanoparticle−ligand complex (NLC) with a hydrophobic surface can well be formed (see Figure 1c). Before placing the NLC in the membrane−water system, we first check its stability in water. As shown in Figure S5 of Supporting Information, when P_a is large or the time of NLC staying in water is short, the NLC is at least metastable.

We then place the NLC about 0.5 nm above the membrane. Because the complex surface is hydrophobic, it can spontaneously insert into the membrane, which requires about 200 ns. Meanwhile, the amphiphilic ligands begin to break off due to the mass reaction, and they prefer to enter into the bilayer and arrange along the lipid distribution. Once the ligands are apart from the nanoparticle causing the decrease of the ligand concentration around nanoparticle, the reverse reaction (bond-breaking) will predominate in the balance according to Le Chatelier's Principle.[29] This is why the ligands can totally detach from the nanoparticle, differing from the situations in oil or water. Since the hydrophilic nanoparticle does not like to stay in the hydrophobic environment inside the bilayer, it tends to leave the bilayer with some ligands detaching from the nanoparticle (see Figure 1d). Finally, the nanoparticle may be driven out of the bilayer *via* the upper or lower leaflets because of hydrophobic interaction. The whole penetration process of the NLC undergoes four stages (see Figure S6 in Supporting Information) *via* its interacting with the membrane, inserting inside the bilayer, leaving (but still sticking to) the bilayer, and finally detaching from the membrane.

Because of the mirror symmetry of membrane along the *z* direction, theoretically speaking, the probability of the spherical nanoparticle's successful penetration should be 50%. Interestingly, we perform 50 independent runs by changing random numbers or initial conformations in the simulations, 30 simulations of which occur successfully. Even if we change the parameters like P_{on}, the resulting penetration efficiency is still larger than 50%. This is due to the fact that, when NLC begins to enter into the membrane, the ligands interacting with the membrane are easier to detach from the nanoparticle than those still in water. Therefore, when the NLC stays inside the bilayer, the ligand

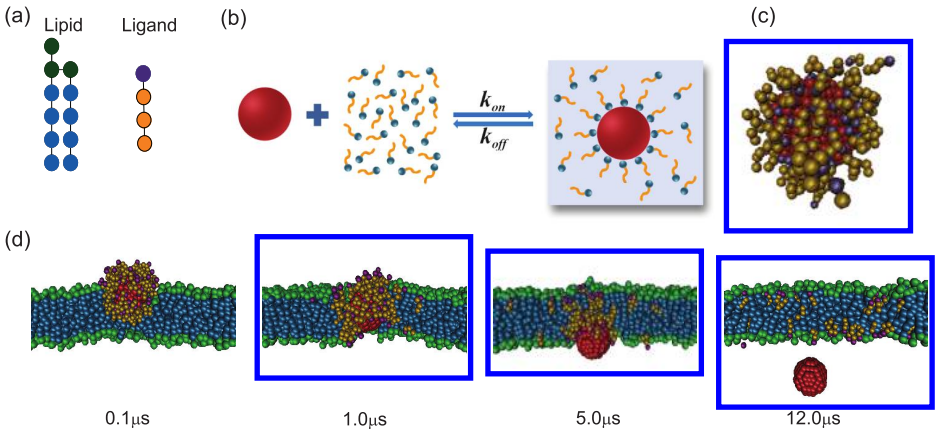

Figure 1. (a) Architecture of lipid and ligand molecules. Green, head beads of lipid; blue, tail beads of lipid; purple, hydrophilic head of ligand; orange, hydrophobic beads of ligand. (b) Schematic representation of the equilibrium between nanoparticle and ligands, where k_{on} and k_{off} denote on-rate and off-rate constant for forming a nanoparticle−ligand complex (NLC), respectively. (c) Snapshot of self-assembled NLC in the oil (oil beads are omitted). (d) Snapshots of four stages of the NLC interacting with the lipid bilayer, where the nanoparticle diameter is 3 nm and the surface ligand density is 3.0 nm^{-2}.

number of the upper surface is larger than that of the lower surface on the nanoparticle, which makes the nanoparticle more likely to leave the bilayer through the lower leaflet. In the following simulations, unless otherwise stated, the type of dynamic bond ($P_{on} = 0.50$ and $P_a = 40$) and the diameter of spherical nanoparticle (3 nm) will be kept unchanged.

Effect of the Surface Decoration of Ligands. The nanoparticle surface plays an important role in its interaction with membranes.[5,7,30] The surface property of the NLC will greatly depend on the density and type of decorated ligands. The ligand number is a key design parameter of NLC.[31] For a given particle size, increasing the ligand density, σ, will make the surface more hydrophobic so that the NLC can easily enter into the bilayer. On the contrary, a decrease in the ligand number may suppress the entry of NLC into the bilayer. This is because, as the NLC interacts with the membrane, most ligands are detached from the nanoparticle and the surface becomes almost hydrophilic. As a consequence, the NLC may not enter into the bilayer. In our simulation, six kinds of NLCs with different σ values are listed. Figure 2a shows that the penetration efficiency increases with increasing the ligand density σ when $\sigma < 3.0$ nm^{-2}, and the maximum penetration efficiency is about 60% and approximately remains the same even when $\sigma > 3.0$ nm^{-2}. However, as shown in Figure 2b, translocation time increases monotonously with σ since more ligands will need more time for the breakdown of dynamic bonds. Therefore, there may exist an optimal ligand density σ_{opt} for nanoparticle penetration, and in the present case, $\sigma_{opt} \approx 3.0$ nm^{-2}, where the penetration efficiency is the highest while translocation time is not very long.

Now we examine the effect of the type of dynamic bond on penetration efficiency and translocation time by varying P_a and P_{on}. The two limiting cases correspond to $P_a = 0$ and ∞, respectively. When $P_a = 0$ (*i.e.*, $P_{on} = 0$ while $P_{off} \neq 0$), the dynamic bond cannot be formed, and thus the NLC surface is still hydrophilic so that it just attaches to the membrane, similar to the case in Figure S2.a of Supporting Information. On the other hand, when $P_a = \infty$ (*i.e.*, $P_{off} = 0$ while $P_{on} \neq 0$), the dynamic bond can be taken as a covalent one, namely, it cannot be broken. Therefore, the NLC surface is hydrophobic, and it will usually stay inside the bilayer (see Figure S2.b in Supporting Information). Next, we will study the general cases. Figure 2c shows the penetration efficiency as a function of P_a, and it can reach almost 60%. The penetration efficiency also depends on P_{on} even for the same P_a. A small P_{on} requires a small P_{off} in the fixed P_a, which reduces the breakdown of dynamic bonds before entering the bilayer. As a result, the NLC with smaller P_{on} (or P_{off}) has a greater probability of entering into the bilayers so that the penetration efficiency becomes higher. However, the translocation time increases with decreasing P_{on} (or P_{off}) for the same P_a due to the slowing down of bond-breaking within the bilayer, shown in Figure 2d. For sufficiently large P_a (namely, P_{off} is very small) that can ensure the entry of nanoparticles into the bilayer, the effect of changing P_{on} (or P_{off}) with the same P_a on the penetration efficiency can be neglected. However, translocation time will increase exponentially with increasing P_a because of the lower breakdown of dynamic bonds within the bilayer (see Figure 2d). Therefore, for large P_a, the time spent for the total penetration process will become very long.

As more and more asymmetric (*e.g.*, Janus and anisotropic shape) nanoparticles can now be prepared in experiments,[32,33] the asymmetric property of nanoparticles becomes increasingly important when interacting with cells.[10,34,35] In our study, a possible way is to break the symmetry of nanoparticle along the *z* direction by asymmetric decoration, which may increase its penetration efficiency. We jointly change the upper (σ_{upper}) and lower (σ_{lower}) ligand surface density on the

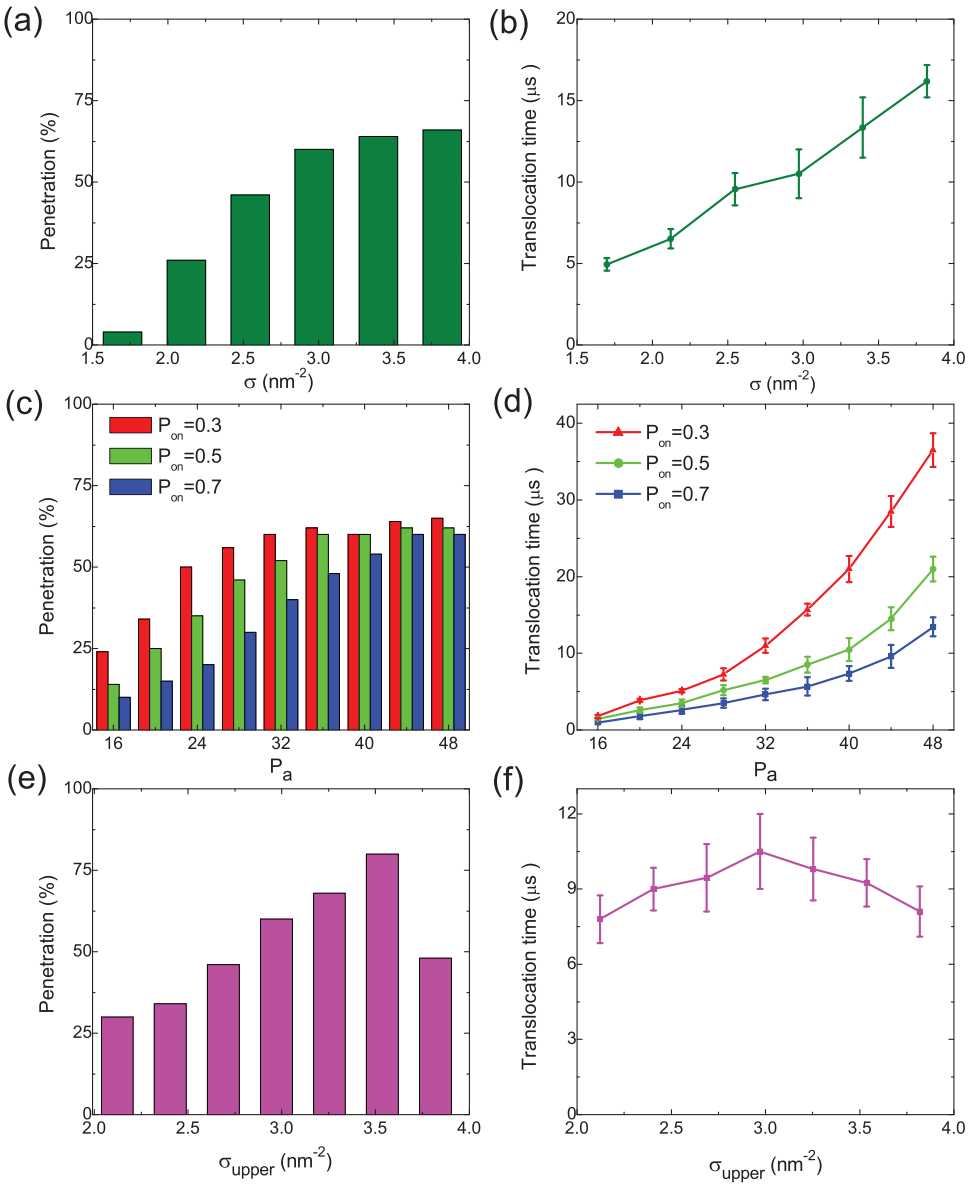

Figure 2. Effect of ligand decoration on the nanoparticle penetration. Penetration efficiency (a) and translocation time (b) as functions of ligand density σ; penetration efficiency (c) and translocation time (d) as functions of P_a with four different values of P_{on} when σ = 3.0 nm^{-2}; penetration efficiency (e) and translocation time (f) as functions of ligand density on the upper surface (σ_{upper}) of nanoparticles, where the total number of ligands is fixed.

nanoparticle but keep the total ligand number unchanged. Figure 2e shows the variation of penetration efficiency with increasing σ_{upper}, and it may even increase to 80% when σ_{upper} = 3.54 nm^{-2} (σ_{lower} = 2.40 nm^{-2}). However, the penetration efficiency will decrease greatly if σ_{lower} is sufficiently small. This is because, when σ_{lower} decreases, the NLC prefers to penetrate across the lower leaflet of membranes, but the sufficiently low σ_{lower} may suppress the entry of the nanoparticle into the membrane and the penetration efficiency will certainly decrease greatly. Additionally, we find from Figure 2f that the maximum of translocation time appears at $\sigma_{upper} = \sigma_{lower}$, and any asymmetric change of upper or lower surface densities will lower the translocation time. This is because the surface of relatively small ligand density, which is favorable to water, will accelerate the escape of nanoparticles from the bilayer.

Effect of the Property of Nanoparticles. The nanoparticle size is an important factor in its penetration through membranes.[12,13,31] Here we examine the penetration ability of the nanoparticle by varying its diameter (2.1, 3.0, 3.9, and 4.8 nm) when the ligand number and density are fixed, respectively. Figure 3a,b compares the penetration efficiency and translocation time by varying the nanoparticle size for the same ligand number N = 84. We find that the penetration efficiency decreases by increasing the nanoparticle size and is only 5% when the nanoparticle size is 4.8 nm. For a larger nanoparticle, we think it may be impossible to

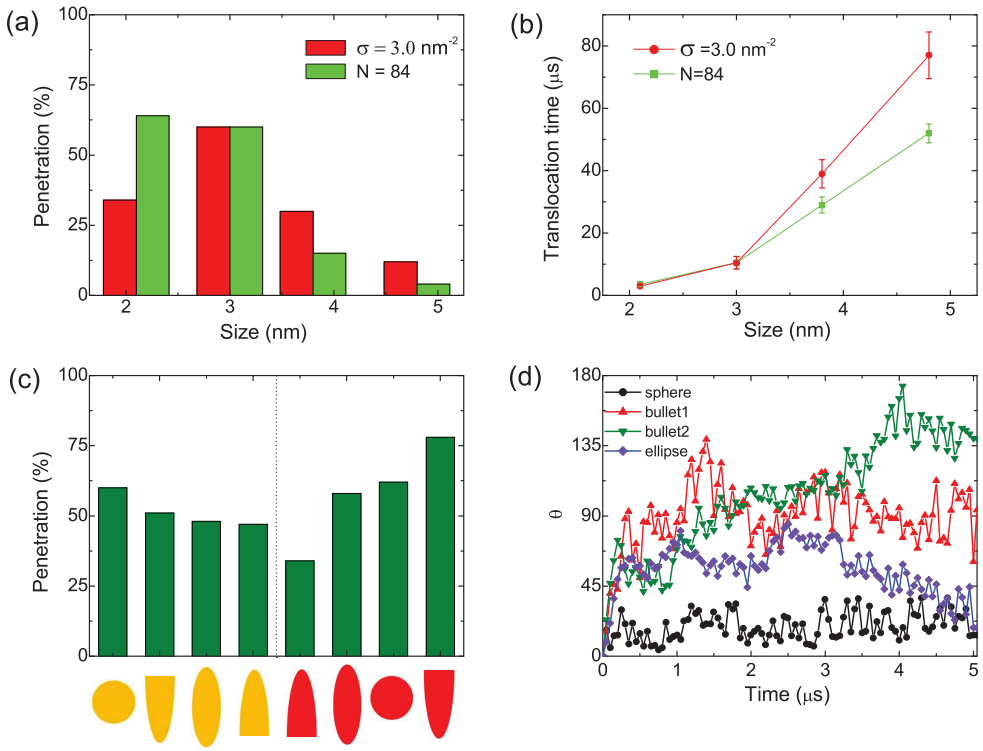

Figure 3. Effect of the property of nanoparticles on their penetration efficiency and translocation time. (a) Penetration efficiency and (b) translocation time as a function of the nanoparticle size. Red line shows the case of the same ligand surface density, while green line denotes the same ligand number on the surface. (c) Penetration efficiency of nanoparticles with different shapes and fixed volume (ellipse with half lengths of 1.05, 1.05, and 3.0 nm in three axes; sphere with radius of 1.5 nm; bullet with half lengths of 1.2, 1.2, and 4.5 nm in three axes). The orange nanoparticles can rotate freely, while the rotation of red nanoparticles is fixed during the penetration process. (d) Time evolution of different (orange) nanoparticles' orientations during the penetration processes.

penetrate through membranes. This is because, with the increase of the nanoparticle size, ligand density σ decreases (namely, the hydrophobic degree of the NLC decreases). When σ is so low that NLC cannot enter into the membrane, the penetration efficiency will become very low. Additionally, the translocation time will become larger with an increase of the nanoparticle size because the decrease of excluded volume effect in low σ increases the bond-breaking time of the NLC. For the same σ ($\sim$3 nm^{-2}) with varying sizes, bond-breaking time of single ligand is approximately the same at the beginning. However, the detachment of the same ligand number from nanoparticles will lead to the different σ with variation of the nanoparticle size. For a smaller nanoparticle, the influence will become more obvious. As a result, the penetration efficiency of the 2.1 nm particle decreases because the ligand number is not enough to make it insert into membranes, as shown in Figure 3a. However, Figure 3a also shows that penetration efficiency decreases when the particle size is larger than 3.0 nm. This is because larger particles (*e.g.*, their complexes are about twice as thick as membranes' thickness) cause the large deformation of the membrane so that it is harder for them to enter into membranes even for high σ. Figure 3b shows that translocation time increases with the increase of nanoparticle size, accompanied by the existence of more dynamic bonds. In the present case, the optimal nanoparticle size may be 3.0 nm.

The shape of nanoparticles is an another important factor affecting the penetration efficiency.[10] The shape anisotropy of nanoparticles plays a very complicated role in their translocation because it can break the symmetry of the system along the penetrating direction, similar to the case of asymmetric decoration of nanoparticles. To clarify this effect, the initial long-axis orientation of nanoparticles with different shapes is required to be along the bilayer normal. In this sense, elliptical particles may not increase the penetration efficiency because they are symmetric in the *z* direction. Instead, their efficiency will become lower ($\sim$50%) because of the rotation of anisotropic nanoparticles during the penetration process, compared to that ($\sim$60%) of the spherical particles (Figure 3c,d). If its rotation is fixed, the penetration efficiency of the elliptical nanoparticle will be nearly 60%. In order to break the symmetry in the *z* direction, we prepare bullet-like nanoparticles and consider two different initial orientations: ▼ and ▲. If we do not constrain its rotation, the penetration efficiency is just about 50% in the two cases. If the rotation is fixed, Figure 3c shows that penetration efficiency in the former case (▼) will

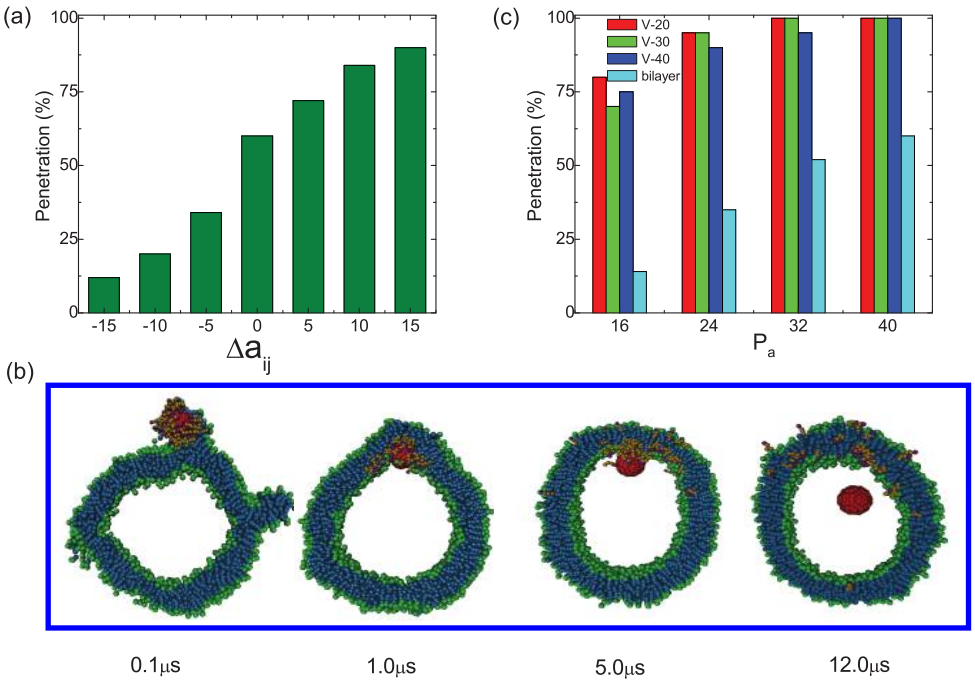

Figure 4. Effect of composition- and curvature-dependent membrane asymmetry on the nanoparticle penetration. (a) Penetration efficiency as a function of Δa_{ij} for the composition-dependent asymmetric bilayer, where Δa_{ij} is the difference between the interactions of upper and lower lipid leaflets with ligand tails of the nanoparticle. For the curved membrane case: (b) time evolution of snapshots of the nanoparticle penetrating through the vesicle where the nanoparticle diameter is 3 nm, the surface ligand density is 3.0 nm^{-2}, and the vesicle diameter is 20 nm; and (c) penetration efficiency as a function of P_a with four different kinds of membranes where the vesicle diameter is 20, 30, 40 nm, and ∞ (*i.e.*, planar lipid bilayers).

increase to about 80% and decrease to about 30% in the latter case (▲). In summary, the rotation may suppress the biased delivery of nanoparticles across two leaflets; therefore, the penetration efficiency remains ~50%. On the other hand, by fixing the rotation of asymmetric bullet-like nanoparticles, we can greatly enhance or suppress their delivery efficiency, depending on the initial (▼ and ▲) orientation. Interestingly, such a process may be realized by adjusting the upper (σ_{upper}) and lower (σ_{lower}) surface densities of ligands on spherically symmetric nanoparticles. Actually, a comparison of Figure 3c and Figure 2e can show that the penetration efficiency of bullet-like nanoparticles with fixed orientation ▼ and ▲ is equivalent to that of spherical nanoparticles with $\sigma_{upper} \approx 3.54$ nm^{-2} and $\sigma_{upper} \approx 2.40$ nm^{-2}, respectively.

Interactions of Nanoparticles with Asymmetric Membranes. Real biomembranes that contain different lipid species and proteins have complicated structures,[36] which always present composition- and curvature-dependent lipid asymmetry. Therefore, studying the interactions between nanoparticles and asymmetric membranes is vitally important and may have many significant applications. For composition-dependent asymmetric membranes arising from different lipid species in two leaflets of the planar bilayer,[19,37] we introduce the difference Δa_{ij} between the interactions of upper and lower lipid leaflets with ligand tails of the nanoparticle to distinguish two kinds of lipid species. Figure 4a shows that the penetration efficiency increases monotonously with increasing the asymmetric degree (*i.e.*, Δa_{ij}) of bilayers. When the value of Δa_{ij} is 15, penetration efficiency has already reached ~90%, which is larger than the highest efficiency in the case of asymmetric decoration of nanoparticles. Therefore, the composition asymmetry of membranes may facilitate the nanoparticle penetration. We also examine different interactions between upper and lower lipid leaflets and nanoparticle beads in our simulations and find that the penetration efficiency remains almost unchanged. As illustrated in Figure 1d, the nanoparticle which is surrounded by ligands has little chance to interact with lipid tails. So, the interaction between nanoparticles and lipid tails is not very important during the penetration pocess. By contrast, the ligands directly interact with lipid tails in the first three stages, and therefore, changing the interaction parameter between them can affect the penetration efficiency obviously. This "amazing" result may give some useful suggestions on drug delivery: although we cannot change the type of nanoparticles during their delivery into cells, we can change the type of ligands to sufficiently utilize the membrane asymmetry and promote nanoparticle penetration into cells.

To elucidate the effect of curvature-dependent membrane asymmetry, we construct vesicles with different diameters to generate curved membranes. Since the area per lipid is the same, the lipid number in the outer leaflet of a vesicle is larger than that in the

inner leaflet. Thus, after the NLC enters into the curved bilayer, the interaction of the NLC with the outer lipid leaflet becomes relatively stronger, which tends to drive the NLC to enter into the vesicle interior across the inner lipid leaflet (see Figure 4b). Therefore, we conclude that penetration efficiency of nanoparticles across asymmetric curved membranes is higher than that across planar membranes. Figure 4c shows the penetration efficiency as a function of P_a by using vesicles of different sizes. Here, the effect of P_a assisting nanoparticle entry into the bilayer becomes less obvious compared to the case of the planar membrane because nanoparticles are easily surrounded by lipids under the deformation of an asymmetrically curved membrane. The highest efficiency may be close to 100% when $P_a > 32$. We also perform the simulations when the NLC is initially placed in the interior of the vesicle, and the penetration efficiency of the particle through the outer leaflet is smaller than 10% (see Figure S7 in Supporting Information), again indicating that the high penetration in the present case is due to the difference in lipid number of inner and outer leaflets. It is now realized that the curved membrane structures, such as buds and tubules in a cell, are essential to many cellular functions such as endocytic trafficking and pathways.[38] The present result shows important evidence that the curved membrane structures may greatly facilitate the entry of nanoparticles into cells.

CONCLUSIONS

We have successfully designed one new type of nanoparticles that can spontaneously penetrate through membranes by adopting a reversible reaction between nanoparticle and ligands. It is found that the properties of ligands and nanoparticles constructing the nanoparticle−ligand complex (NLC) can affect their penetration efficiency and translocation time, and especially for nanoparticles with anisotropic shape or asymmetric surface decoration, the penetration efficiency can reach about 80% when NLC has the effective bullet-like shape oriented in a certain direction. Furthermore, we provide insights into the interaction between nanoparticles and asymmetric membranes and find that the membrane asymmetry can highly affect the nanoparticle penetration and increase the penetration efficiency to above 90% under proper situations.

Finally, we point out the feasibility and application of our novel nanoparticles in real experiment. Generally, the idea for designing this type of novel nanoparticles is on the basis of nanoparticle−ligand dynamics, which can be regulated by the local hydrophobic−lipophilic interactions. To some extent, the key idea is similar to that of stimuli materials like pH-sensitive, thermo-sensitive, and light-sensitive materials in experiments,[39,40] where the chemical properties of those materials are changed by external stimulus. The present model may give some hints for designing this type of novel nanoparticles in experiment as stimulus materials, namely, how to design the type of dynamic bond of nanoparticles, whose stability depends on change in environments (*e.g.*, pH) inside/outside cell membranes, to realize the high penetration efficiency. Therefore, we believe that this type of novel nanoparticles could be engineered with the advance of nanotechnology in the future, and their high penetration efficiency as well as low toxicity, though still need to be evaluated by biomedicinal scientists, will make it a potentially huge application in drug/gene delivery.

METHODS

Dissipative particle dynamics (DPD) is a coarse-grained simulation technique with hydrodynamic interaction.[41−43] The dynamics of the elementary units, which are so-called DPD beads, is governed by Newton's equation of motion: $d\mathbf{v}_i/dt = \mathbf{f}_i/m$. In DPD, there are three types of pairwise forces acting on bead i by bead j:[43] the conservative force $\mathbf{F}_{ij}^C$, dissipative force $\mathbf{F}_{ij}^D$, and random force $\mathbf{F}_{ij}^R$. The conservative force is taken as $\mathbf{F}_{ij}^C = a_{ij}(1 - r_{ij}/r_c)\hat{\mathbf{e}}_{ij}$ with the cutoff radius r_c, where $\mathbf{r}_{ij} = \mathbf{r}_i - \mathbf{r}_j$, $r_{ij} = |\mathbf{r}_{ij}|$, and $\hat{\mathbf{e}}_{ij} = \mathbf{r}_{ij}/r_{ij}$. The parameter a_{ij} represents the maximum repulsion interaction of beads of type i and type j. The dissipative force is $\mathbf{F}_{ij}^D = -\gamma(1 - r_{ij}/r_c)(\hat{\mathbf{e}}_{ij} \cdot \mathbf{v}_{ij})\hat{\mathbf{e}}_{ij}$, where $\mathbf{v}_{ij} = \mathbf{v}_i - \mathbf{v}_j$ is relative velocity between beads i and j, and γ is the strength of friction. The random force takes the form of $\mathbf{F}_{ij}^R = (2\gamma k_B T)^{1/2}(1 - r_{ij}/r_c)\zeta_{ij}\Delta t^{-1/2}\hat{\mathbf{e}}_{ij}$. Here, ζ_{ij} is a symmetric random variable with zero mean and unit variance, namely, $\langle\zeta_{ij}(t)\rangle = 0$ and $\langle\zeta_{ij}(t)\zeta_{kl}(t')\rangle = (\delta_{ik}\delta_{jl} + \delta_{il}\delta_{jk})(\delta(t - t'))$. Δt is the time step of simulation.

In order to ensure the integrality of lipids and ligands, the harmonic spring interaction $\mathbf{F}_s = -k_s(1 - r_{i,i+1}/l_0)\hat{\mathbf{e}}_{i,i+1}$ is applied between neighboring beads in a single molecule, where k_s is the spring constant and l_0 is the equilibrium bond length. We use $k_s = 128$ and $l_0 = 0.5$ between the neighboring beads, and a weak bond ($k_s = 20$ and $l_0 = 0.5$) is inserted between the second hydrophobic beads on two tails to keep the tails oriented in the same direction.[30] For ligands, we use $k_s = 128$ and $l_0 = 0.5$, and for dynamic bond, $k_s = 20$ and $l_0 = 0.5$ are used. The rigidity of lipid tails is denoted by a three-body bond angle potential $U_a = k_a(1 - \cos(\varphi - \varphi_0))$, where φ is the angle formed by three adjacent beads in the same tail and φ_0 is the equilibrium value of the angle. We set the coefficients $k_a = 10$ and $\varphi_0 = 180°$. In order to denote the hydrophilic/hydrophobic property of the beads, for any two beads of the same type, we take the repulsive parameter $a_{ii} = 25$, and for any two beads of different types, we set the interaction parameter $a_{HW} = a_{HP} = a_{HL} = a_{TN} = a_{WP} = a_{WL} = a_{ON} = 25$ and $a_{HT} = a_{HN} = a_{TW} = a_{TP} = a_{TL} = a_{WN} = a_{OP} = a_{OL} = a_{PN} = a_{LN} = 100$,[30] where W stands for the water bead, H stands for the lipid head bead, T stands for the lipid tail bead, O stands for the oil bead, P stands for the bead of the nanoparticle, L stands for the hydrophilic bead of the ligand, and N stands for hydrophobic bead of the ligand. Additionally, we set $a_{PL} = 20$, meaning that the nanoparticle is favorable to ligands. To gain the high ligand density on the nanoparticle surface, the radius of ligand beads is set as $0.8r_c$. The other beads have the same radius of r_c.[44]

Our simulations apply the velocity−Verlet integration algorithm and the integration time step $\Delta t = 0.02\tau$. In addition, we choose the cutoff radius r_c, bead mass m, and energy k_BT as the simulation units. All simulations are performed in the NVT

ensembles. The size of the simulation box is 40 × 40 × 40 with the number density of $\rho = 3$. There is a total of 192 000 DPD beads in our simulation box, and the periodic boundary conditions are adopted in three directions. All simulations in this work are carried out by using the soft package Lammps (15 Jan 2010).[45]

Acknowledgment. This work was supported by the National Natural Science Foundation of China under Grants 91027040 and 10974080, the National Basic Research Program of China (No. 2012CB821500), and the Project Funded by the Priority Academic Program Development of Jiangsu Higher Education Institutions. We are grateful to the High Performance Computing Center (HPCC) of Nanjing University for doing the numerical calculations in this paper on its IBM Blade cluster system.

Supporting Information Available: The formation of lipid membranes and their interactions with hydrophilic and hydrophobic nanoparticles, the formation of nanoparticle−ligand complex (NLC) in oil, the stability of NLC in water, and the additional figures of the interactions between NLC and membranes. This material is available free of charge *via* the Internet at http://pubs.acs.org.

REFERENCES AND NOTES

1. Boyer, C.; Bulmus, V.; Davis, T. P.; Ladmiral, V.; Liu, J. Q.; Perrier, S. Bioapplications of RAFT Polymerization. *Chem. Rev.* **2009**, *109*, 5402–5436.
2. Xia, Y. N. Nanomaterials at Work in Biomedical Research. *Nat. Mater.* **2008**, *7*, 758–760.
3. Sanhai, W. R.; Sakamoto, J. H.; Canady, R.; Ferrari, M. Seven Challenges for Nanomedicine. *Nat. Nanotechnol.* **2008**, *3*, 242–244.
4. Rajendran, L.; Knolker, H. J.; Simons, K. Subcellular Targeting Strategies for Drug Design and Delivery. *Nat. Rev. Drug Discovery* **2010**, *9*, 29–42.
5. Nel, A. E.; Madler, L.; Velegol, D.; Xia, T.; Hoek, E. M. V.; Somasundaran, P.; Klaessig, F.; Castranova, V.; Thompson, M. Understanding Biophysicochemical Interactions at the Nano-Bio Interface. *Nat. Mater.* **2009**, *8*, 543–557.
6. Mitragotri, S.; Lahann, J. Physical Approaches to Biomaterial Design. *Nat. Mater.* **2009**, *8*, 15–23.
7. Verma, A.; Stellacci, F. Effect of Surface Properties on Nanoparticle−Cell Interactions. *Small* **2010**, *6*, 12–21.
8. Leroueil, P. R.; Hong, S.; Mecke, A.; Baker, J. R.; Orr, B. G.; Holl, M. M. B. Nanoparticle Interaction with Biological Membranes: Does Nanotechnology Present a Janus Face? *Acc. Chem. Res.* **2007**, *40*, 335–342.
9. Ginzburg, V. V.; Balijepalli, S.; Smith, K. A.; Balazs, A. C. Approaches to Mesoscale Modeling of Nanoparticle−Cell Membrane Interactions. In *Nanotechnologies for the Life Sciences: Nanostructured Oxides*; Wiley-VCH: Weinheim, Germany, 2009; Vol. 2, pp 317−355.
10. Yang, K.; Ma, Y. Q. Computer Simulation of the Translocation of Nanoparticles with Different Shapes Across a Lipid Bilayer. *Nat. Nanotechnol.* **2010**, *5*, 579–583.
11. Verma, A.; Uzun, O.; Hu, Y. H.; Hu, Y.; Han, H. S.; Watson, N.; Chun, S. L.; Irvine, D. J.; Stellacci, F. Surface-Structure-Regulated-Cell-Membrane Penetration by Monolayer-Protected Nanoparticles. *Nat. Mater.* **2008**, *7*, 588–595.
12. Gao, H. J.; Shi, W. D.; Freund, L. B. Mechanics of Receptor-Mediated Endocytosis. *Proc. Natl. Acad. Sci. U.S.A.* **2005**, *102*, 3213–3218.
13. Zhang, S. L.; Li, J.; Lykotrafitis, G.; Bao, G.; Suresh, S. Size-Dependent Endocytosis of Nanoparticles. *Adv. Mater.* **2009**, *21*, 419–424.
14. Smith, K. A.; Jasnow, D.; Balazs, A. C. Designing Synthetic Vesicles That Engulf Nanoscopic Particles. *J. Chem. Phys.* **2007**, *127*, 084703.
15. Roiter, Y.; Ornatska, M.; Rammohan, A. R.; Balakrishnan, J.; Heine, D. R.; Minko, S. Interaction of Nanoparticles with Lipid Membrane. *Nano Lett.* **2008**, *8*, 941–944.
16. Jin, H.; Heller, D. A.; Sharma, R.; Strano, M. S. Size-Dependent Cellular Uptake and Expulsion of Single-Walled Carbon Nanotubes: Single Particle Tracking and a Generic Uptake Model for Nanoparticles. *ACS Nano* **2009**, *3*, 149–158.
17. Rasmussen, J. P. R; Riviere, J. E.; Riviere, N. A. M. Variables Influencing Interactions of Untargeted Quantum Dot Nanoparticles with Skin Cells and Identification of Biochemical Modulators. *Nano Lett.* **2007**, *7*, 1344–1348.
18. Chen, X.; Kis, A.; Zettl, A.; Bertozzi, C. R. A Cell Nanoinjector Based on Carbon Nanotubes. *Proc. Natl. Acad. Sci. U.S.A.* **2007**, *104*, 8218–8222.
19. Gurtovenko, A. A.; Anwar, J.; Vattulainen, L. Defect-Mediated Trafficking Across Cell Membranes: Insights from Silico Modeling. *Chem. Rev.* **2010**, *110*, 6077–6103.
20. Ting, C. L.; Wang, Z. G. Interactions of a Charged Nanoparticle with a Lipid Membrane: Implications for Gene Delivery. *Biophys. J.* **2011**, *100*, 1288–1297.
21. Lee, H; Larson, R. G. Multiscale Modeling of Dendrimers and Their Interactions with Bilayers and Polyelectrolytes. *Molecules* **2009**, *14*, 423–438.
22. Ginzburg, V. V.; Balijepalli, S. Modeling Thermodynamics of Nanoparticle Interactions with Cell Membranes. *Nano Lett.* **2007**, *7*, 3716–3722.
23. Li, Y.; Chen, X.; Gu, N. Computational Investigation of Interaction between Nanoparticles and Membranes: Hydrophobic/Hydrophilic Effect. *J. Phys. Chem. B* **2008**, *112*, 16647–16653.
24. Qiao, R.; Roberts, A. P.; Mount, A. S.; Klaine, S. J.; Ke, P. C. Translocation of C_{60} and Its Derivatives Across a Lipid Bilayer. *Nano Lett.* **2007**, *7*, 614–619.
25. Pogodin, S.; Baulin, V. A. Can a Carbon Nanotube Pierce through a Phospholipid Bilayer? *ACS Nano* **2010**, *4*, 5293–5300.
26. Rasch, M. R.; Rossinyol, E.; Hueso, J. L.; Goodfellow, B. W.; Arbiol, J.; Korgel, B. A. Hydrophobic Gold Nanoparticle Self-Assembly with Phosphatidylchline Lipid: Membrane-Loaded and Janus Vesicles. *Nano Lett.* **2010**, *10*, 3733–3739.
27. Wojtecki, R. J.; Meador, M. A.; Rowan, S. J. Using the Dynamic Bond To Access Macroscopically Responsive Structually Dynamic Polymers. *Nat. Mater.* **2011**, *10*, 14–27.
28. Bongrand, P. Ligand-Receptor Interactions. *Rep. Prog. Phys.* **1999**, *62*, 921–968.
29. Atkins, P. W. *The Elements of Physical Chemistry*, 3rd ed.; Oxford University Press: Oxford, 1993; pp 114−115.
30. Alexeev, A.; Uspal, W. E.; Balazs, A. C. Harnessing Janus Nanoparticles To Create Controllable Pores in Membranes. *ACS Nano* **2008**, *2*, 1117–1122.
31. Wang, S. H.; Dormidontova, E. E. Nanoparticle Design Optimization for Enhanced Targeting: Monte Carlo Simulations. *Biomacromolecules* **2010**, *11*, 1785–1795.
32. Wang, B. B.; Li, B.; Zhao, B.; Li, C. Y. Amphiphilic Janus Gold Nanoparticles *via* Combining "Solid-State Grafting-to" and "Grafting-from" Method. *J. Am. Chem. Soc.* **2008**, *130*, 11594–11595.
33. Glotzer, S. C.; Solomon, A. M. J. Anisotropy of Building Blocks and Their Assembly into Complex Structures. *Nat. Mater.* **2007**, *6*, 557–562.
34. Gratton, S. E. A.; Ropp, P. A.; Pohlhaus, P. D.; Luft, J. C.; Madden, V. J.; Napier, M. E.; DeSimone, J. M. The Effect of Particle Design on Cellular Internalization Pathways. *Proc. Natl. Acad. Sci. U.S.A.* **2008**, *105*, 11613–11618.
35. Chithrani, B. D.; Ghazani, A. A.; Chan, W. C. W. Determining the Size and Shape Denendence of Gold Nanoparticle Uptake into Mammalian Cells. *Nano Lett.* **2006**, *6*, 662–668.
36. Escriba, P. V.; Gonzalez-Ros, J. M.; Goni, F. M.; Kinnunen, P. K. J.; Vigh, L.; Sanchez-Magraner, L.; Fernandez, A. M.; Busquets, X.; Horvath, I.; Coblijn, B. G. Membranes: A Meeting Point for Lipids, Proteins and Therapies. *J. Cell. Mol. Med.* **2008**, *12*, 829–875.
37. Martin, S. E.; Risselada, H. J.; Salgado, J.; Marrink, S. J. Stability of Asymmetric Lipid Bilayers Assessed by Molecular Dynamics Simularions. *J. Am. Chem. Soc.* **2009**, *131*, 15194–15202.
38. Sens, P.; Johannes, L.; Bassereau, P. Biophysical Approches to Protein-Induced Membrane Deformation in Trafficking. *Curr. Opin. Cell Biol.* **2008**, *20*, 1–7.
39. Lowik, D. W. P. M; Leunissen, E. H. P.; Heuvel, M. V. D.; Hansen, M. B.; Hest, J. C. M. V. Stimulus Responsible

Peptide Based Materials. *Chem. Soc. Rev.* **2010**, *39*, 3394–3412.
40. Lee, H. I.; Pietrasik, J.; Sheiko, S. S.; Matyjaszewski, K. Stimuli-Responsive Molecular Brushes. *Prog. Polym. Sci.* **2010**, *35*, 24–44.
41. Hoogerbrugge, P. J.; Koelman, J. M. V. A. Simulating Microscopic Hydrodynamic Phenomena with Dissipative Particle Dynamics. *Europhys. Lett.* **1992**, *19*, 155–160.
42. Espagnol, P.; Warren, P. Statistical Mechanics of Dissipative Particle Dynamics. *Europhys. Lett.* **1995**, *30*, 191–196.
43. Groot, R. D.; Warren, P. B. Dissipative Particle Dynamics: Bridging the Gap between Atomistic and Mesoscopic Simulations. *J. Chem. Phys.* **1997**, *107*, 4423–4435.
44. Yang, K.; Shao, X.; Ma, Y. Q. Shape Deformation and Fission Route of the Lipid Domain in a Multicomponent Vesicle. *Phys. Rev. E* **2009**, *79*, 051924.
45. Plimpton, S. J. Fast Parallel Algorithms for Short-Range Molecular Dynamics. *J. Comput. Phys.* **1995**, *117*, 1–19.